Cancer Cell, Volume *28*

Supplemental Information

MYC Is a Major Determinant of Mitotic Cell Fate

Caroline Topham, Anthony Tighe, Peter Ly, Ailsa Bennett, Olivia Sloss, Louisa Nelson, Rachel A. Ridgway, David Huels, Samantha Littler, Claudia Schandl, Ying Sun, Beatrice Bechi, David J. Procter, Owen J. Sansom, Don W. Cleveland, and Stephen S. Taylor

Supplemental Data

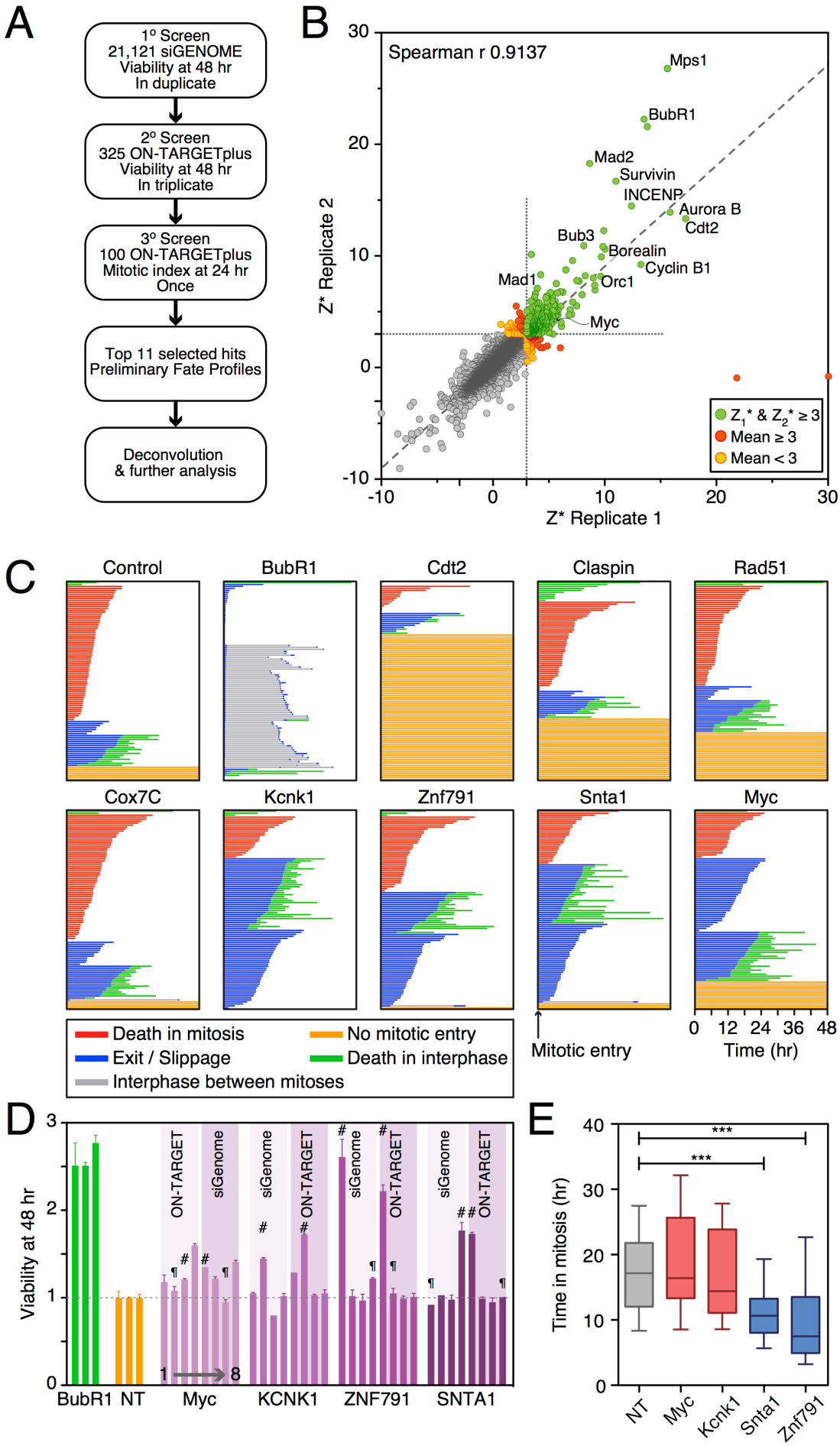

Figure S1, related to Figure 1. A genome-wide siRNA screen for regulators of mitotic cell fate. (**A**) Workflow of the screen. (**B**) Result of the primary screen, plotting the robust Z scores (Z*) for the two replicates. Z* scores were calculated using the median absolute deviation for each plate (Chung et al., 2008). Genes with mean Z* scores greater than 3 were taken forward to the secondary screen. (**C**) Fate profiles of RKO cells transfected with selected ON-TARGETplus SMARTpools and exposed to 0.1 μM taxol. (**D**) Bar graph showing viability of taxol-treated RKO cells after transfection of individual siRNAs from the SMARTpools used in the 1^{o} and 2^{o} screens. While siRNAs in many of the siGENOME and ON-TARGETplus SMARTpools are distinct, in some instances there is duplication, indicated by hashtags (#) and paragraph symbols (¶). Myc siRNAs 4, 5, 6 and 8 repress Myc and inhibit death in mitosis (DiM) (Fig. S2A) so they were pooled and used for further experiments, while #4 was used in isolation for the RNAi-rescue experiment in Fig. S2B. Values represent mean and SD from two experiments. (**E**) Box-and-whisker plots (median, interquartile and 10-90% ranges) showing that in isolation, *SNTA1* #4 and *ZNF791* #1 accelerate mitotic exit. In contrast, the active *KCNK1* siRNA more closely resembles the Myc phenotype.

Table S1, related to Figure 1. Primary screen; MTS values at 48 hr. Used to generate Fig. S1B. (Provided as an Excel file).

Table S2, related to Figure 1. Secondary and tertiary screens; MTS values at 48 hr and mitotic index (granularity) values at 24 hr. Used to generate Fig. 1C. (Provided as an Excel file).

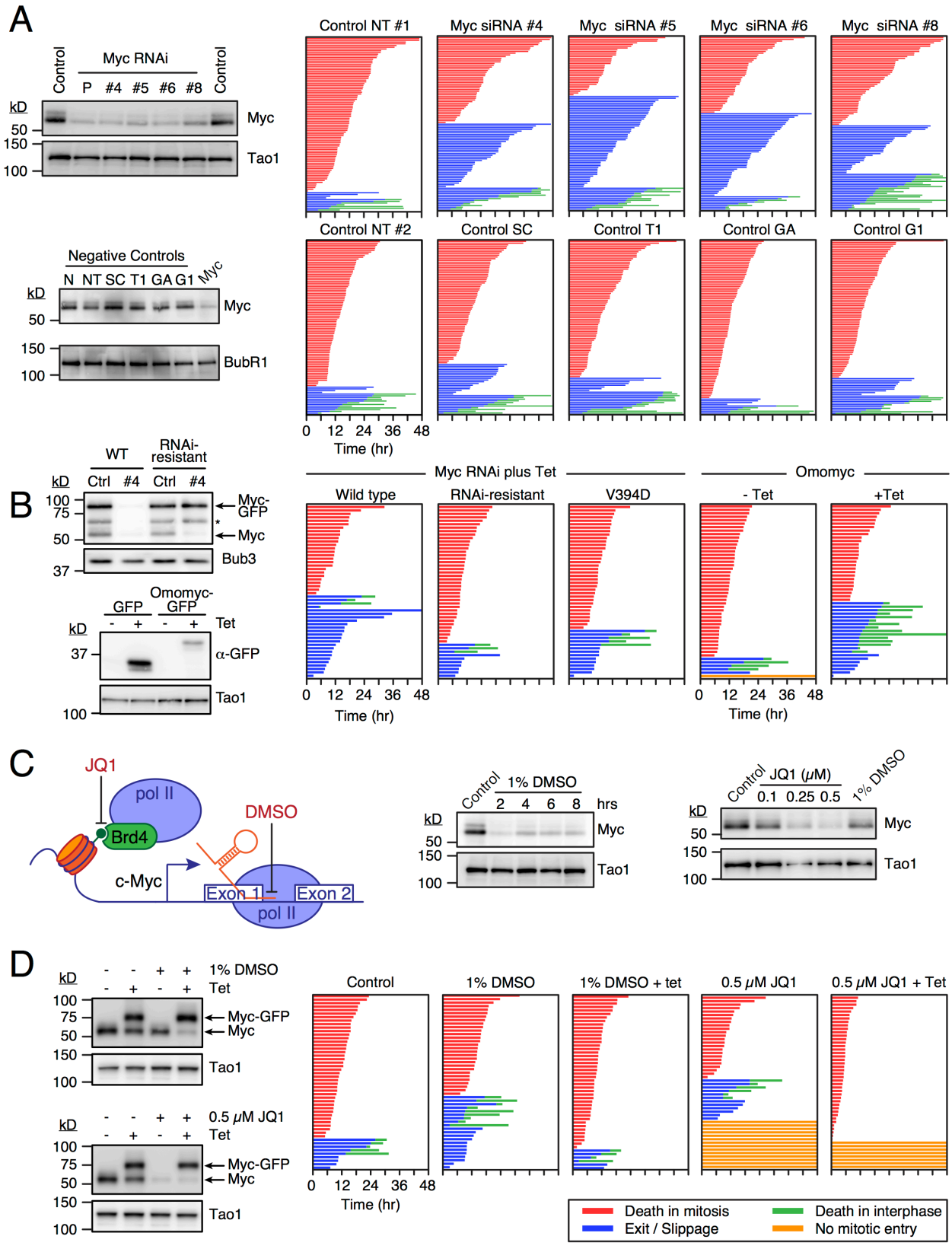

Figure S2, related to Figure 2. Myc is a regulator of mitotic cell fate. (**A**) Deconvolution of siRNA pools targeting Myc. Immunoblots of RKO cells transfected with four active Myc siRNAs, either as a pool (P) or individually (nos 4, 5, 6 and 8), and six negative controls siRNAs. Corresponding fate profiles of transfected RKO cells treated with 100nM taxol. (**B**) Analysis of Myc mutants. Immunoblots show induction of GFP-tagged Myc, an RNAi-resistant mutant and Omomyc in RKO cells treated with 1 µg/ml tetracycline. The asterisk marks a Myc-GFP cleavage product. Fate profiles as in (A). (**C**) Schematic showing how DMSO and JQ1 inhibit transcription of *MYC* and immunoblots confirming that DMSO and JQ1 inhibit Myc in RKO cells. (**D**) Immunoblots and fate profiles showing that a Myc-GFP cDNA is resistant to DMSO and JQ1 and restores the balance back towards death in mitosis.

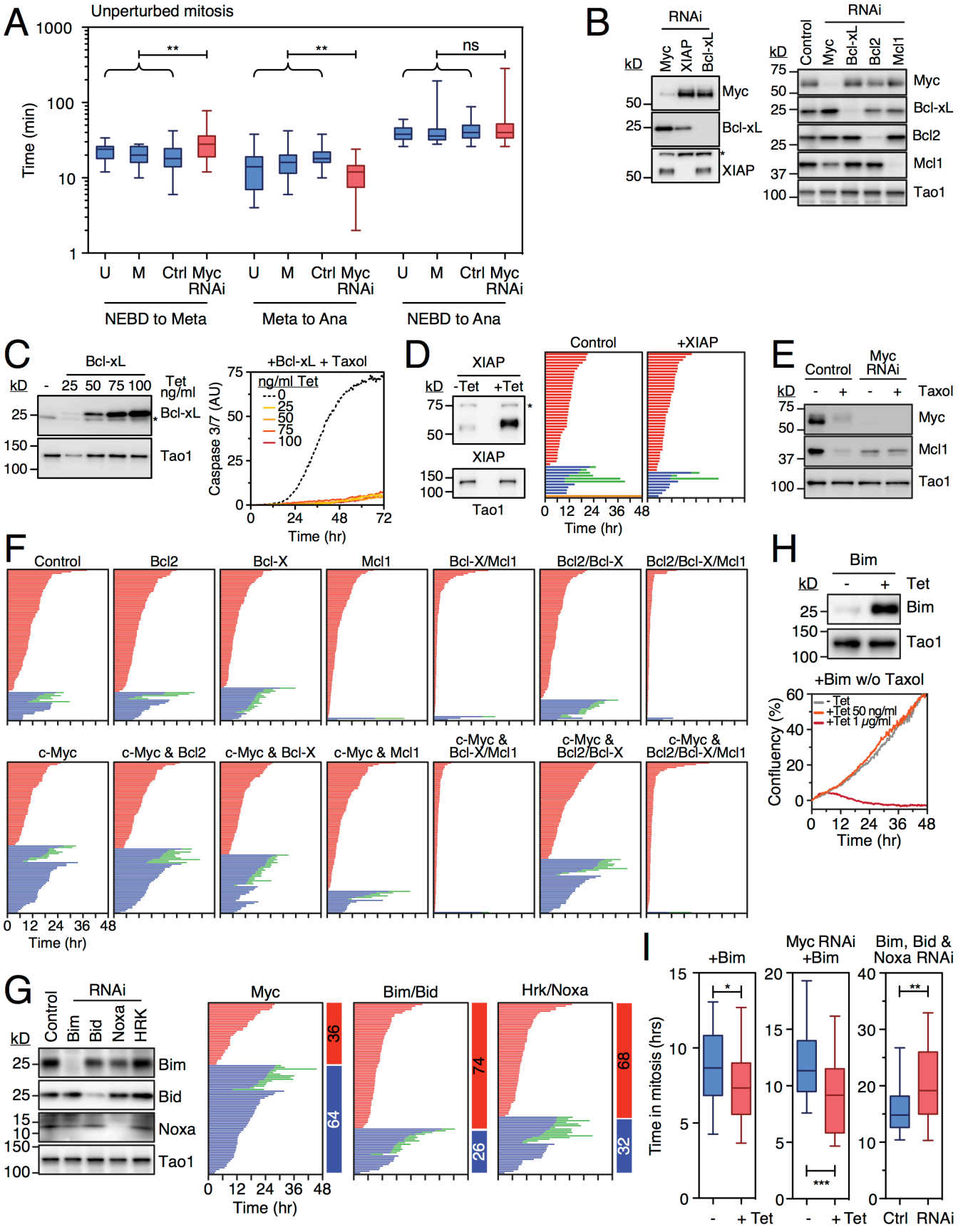
A
Unperturbed mitosis
Time (min)
1000
100
10
1
**
**
ns
U M Ctrl Myc RNAi
U M Ctrl Myc RNAi
U M Ctrl Myc RNAi
NEBD to Meta
Meta to Ana
NEBD to Ana
B
RNAi
Myc XIAP Bcl-xL
kD
Myc
Bcl-xL
XIAP
RNAi
Control Myc Bcl-xL Bcl2 Mcl1
kD
Myc
Bcl-xL
Bcl2
Mcl1
Tao1
C
Bcl-xL
kD - 25 50 75 100 Tet ng/ml
Bcl-xL
Tao1
+Bcl-xL + Taxol
ng/ml Tet
0
25
50
75
100
Caspase 3/7 (AU)
Time (hr)
D
XIAP
kD -Tet +Tet
XIAP
Tao1
Control
+XIAP
Time (hr)
E
Control
Myc RNAi
kD - + - + Taxol
Myc
Mcl1
Tao1
F
Control
Bcl2
Bcl-X
Mcl1
Bcl-X/Mcl1
Bcl2/Bcl-X
Bcl2/Bcl-X/Mcl1
c-Myc
c-Myc & Bcl2
c-Myc & Bcl-X
c-Myc & Mcl1
c-Myc & Bcl-X/Mcl1
c-Myc & Bcl2/Bcl-X
c-Myc & Bcl2/Bcl-X/Mcl1
Time (hr)
H
Bim
kD - + Tet
Bim
Tao1
+Bim w/o Taxol
Confluency (%)
- Tet
+Tet 50 ng/ml
+Tet 1 μg/ml
Time (hr)
G
RNAi
Control Bim Bid Noxa HRK
kD
Bim
Bid
Noxa
Tao1
Myc
Bim/Bid
Hrk/Noxa
36
64
74
26
68
32
Time (hr)
I
+Bim
Myc RNAi +Bim
Bim, Bid & Noxa RNAi
Time in mitosis (hrs)
*
***
**
- + Tet
- + Tet
Ctrl RNAi

Figure S3, related to Figure 3. Analysis of Bcl2-family members. (**A**) Time lapse analysis of RKO cells expressing a GFP-tagged histone H2B, measuring the time from nuclear envelope breakdown (NEBD) to metaphase, from metaphase to anaphase and from NEBD to anaphase. Cells were either untreated (U), mock transfected (M), or transfected with siRNAs, either a non-targeting control (Ctrl) or the pool targeting Myc. Box-and-whisker plots show the median, interquartile ranges and full range. (**B**) Immunoblots showing RNAi-mediated inhibition of Myc, XIAP and pro-survival Bcl2 family proteins in RKO cells. Note that Myc RNAi results in up-regulation of Bcl-xL and down-regulation of Mcl1, but has no obvious effect on XIAP. Asterisk marks a non-specific background band. (**C**) Characterisation of a stable tet-inducible RKO cell line overexpressing Bcl-xL; immunoblot shows induction of Bcl-xL with a range of tetracycline concentrations. Asterisk marks the endogenous protein. Apoptosis assay shows that even low level induction of Bcl-xL is sufficient to block apoptosis induced by taxol. Note that 25ng/ml tetracycline increases Bcl-xL levels only two fold yet this is sufficient to block apoptosis. (**D**) Characterisation of a stable tet-inducible RKO cell line overexpressing XIAP; immunoblot shows induction of XIAP with 1 μg/ml tetracycline. Asterisk marks a non-specific background band. Fate profile shows that tet-induced overexpression of XIAP does not inhibit DiM in 0.1 μM taxol. (**E**) Immunoblot showing reduced Mcl1 levels in Myc RNAi cells. Consistent with Mcl1 being degraded in mitosis, Mcl1 is less abundant in taxol-treated cells. However, Mcl1 levels do not fall further in taxol-treated Myc RNAi cells, possibly due to inhibition of mitotic-specific degradation. (**F**) Fate profiles following RNAi-mediated inhibition of pro-survival Bcl2 family proteins showing that co-repression of Bcl-xL and Mcl1 leads to rapid DiM in 0.1 μM taxol. (**G**) Immunoblots of RKO cells showing RNAi-mediated inhibition of the BH3-only proteins Bim, Bid and Noxa, and fate profiles showing that while Myc RNAi reduces DiM in 0.1 μM taxol to 36% (compared to 69% in the corresponding control shown in Fig. 3D), repressing the BH3-only proteins, either in isolation (not shown) or in pairs as shown here, has little effect, with DiM remaining at ~70%. (**H**) Characterisation of an RKO tet-inducible cell line overexpressing Bim; immunoblot shows induction of Bim with 50 ng/ml tetracycline. The growth curves show that in the absence of taxol, overexpressing Bim to this level alone does not induce apoptosis. (**I**) Box-and-whisker plots (median, interquartile and 10-90 percentile range) showing the time spent arrested in mitosis following overexpression of Bim, either in control cells or following Myc RNAi, and following inhibition of Bim, Bid and Noxa. Note that overexpression of Bim accelerates death in mitosis while inhibition of the three BH3-only proteins delays death.

Table S3, related to Figure 3. Nanostring gene expression profiling data. Used to generate Fig. 3A.

	Common name	Gene Name	Log2 fold change*	Reads
Apoptosis module	AIF	AIFM1	-0.259	429
	Apaf1	APAF1	0.211	263
	ATM	ATM	0.144	59
	BAD	BAD	-0.039	69
	BAK	Bak1	0.125	669
	BAX	BAX	-0.042	756
	Bcl2	BCL2	-0.255	34
	Bcl-XL	BCL2L1	0.477	772
	BimEL	BCL2L11	-0.668	26
	BID	BID	-0.912	187
	cIAP	BIRC3	-0.187	60
	β-TrCP	BTRC	-0.180	194
	Caspase 3	CASP3	0.318	359
	Caspase 7	CASP7	-0.242	261
	Caspase 8	CASP8	-0.167	301
	Casp8a	CASP8AP2	-0.276	191
	Caspase 9	CASP9	0.202	76
	c-FLIP	CFLAR	0.059	124
	CKII	CSNK2B	-0.289	2061
	ICAD	DFFA	-0.753	429
	SMAC	DIABLO	-0.242	193
	E2F1	E2F1	-0.843	316
	Fadd	FADD	0.176	30
	Fbw7	FBW7	-0.408	119
	HRK	HRK	-0.543	17
	Omi	HTRA2	-0.257	80
	MULE	HUWE1	-0.278	767
	p38	MAPK14	0.016	550
	JNK1	MAPK8	-0.282	516
	JNK2	MAPK9	-0.143	546
	Max	MAX	-0.608	681
	Mcl1	MCL1	-0.312	8220
	c-Myc	MYC	-1.085	3168
	Pin1	PIN1	-0.046	245
	NOXA	PMAIP1	-1.080	270
	PKA	PRKACA	0.149	794
	p53	TP53	-0.379	205
	Tradd	TRADD	0.315	17
	Usp9X	USP9X	-0.011	934
	XIAP	XIAP	0.128	327
	MIZ1	ZBTB17	0.223	40

	Common name	Gene Name	Log2 fold change*	Reads
Mitosis module	Apc1	ANAPC1	-0.645	569
	Apc10	ANAPC10	-0.253	193
	Cenp-S	APITD1	-0.602	285
	Aurora A	AURKA	-0.552	1217
	Aurora B	AURKB	-0.513	1315
	Survivin	BIRC5	-0.720	927
	Bub1	BUB1	-0.435	1096
	BubR1	BUB1B	-0.581	799
	Knl1	CASC5	-0.204	498
	Cyclin B1	CCNB1	-0.606	2911
	Cdc20	CDC20	-0.416	1731
	Cdc25	CDC25A	-0.923	632
	Sororin	CDCA5	-0.540	895
	Cdh1	CDK1	-0.514	2734
	Cenp-E	CENPE	-0.332	542
	Cenp-F	CENPF	-0.246	1208
	Cenp-T	CENPT	0.539	16
	Separase	ESPL1	-0.231	337
	Haspin	GSG2	-0.441	396
	Augmin	HAUS1	-0.447	533
	Eg5	KIF11	-0.519	695
	Mad2	MAD2L1	-0.762	1663
	p31 comet	MAD2L1BP	-0.291	643
	Greatwall	MASTL	-0.098	238
	Mis12	MIS12	-0.560	307
	Cap D2	NCAPD2	-0.414	1198
	Cap G	NCAPG	-0.383	763
	Cap H	NCAPH	-0.630	632
	Ndc80	NDC80	-0.331	332
	Nde1	NDE1	-0.395	173
	Plk1	PLK1	-0.579	1647
	Securin	PTTG1	-0.153	112
	Sgo1	SGOL1	-0.167	336
	Ska1	SKA1	-0.331	335
	Smc1	SMC1A	-0.519	278
	Smc2	SMC2	-0.477	473
	Spindly	SPDL1	-0.303	134
	SA2	STAG2	-0.194	730
	Megator	TPR	-0.108	435
	Tpx2	TPX2	-0.460	1236
	Mps1	TTK	-0.517	338
	UbcH10	UBE2C	-0.429	3531
	Wapl	WAPAL	-0.381	779
	Zw10	ZW10	-0.199	266

*Values are the mean of 4 biological replicates

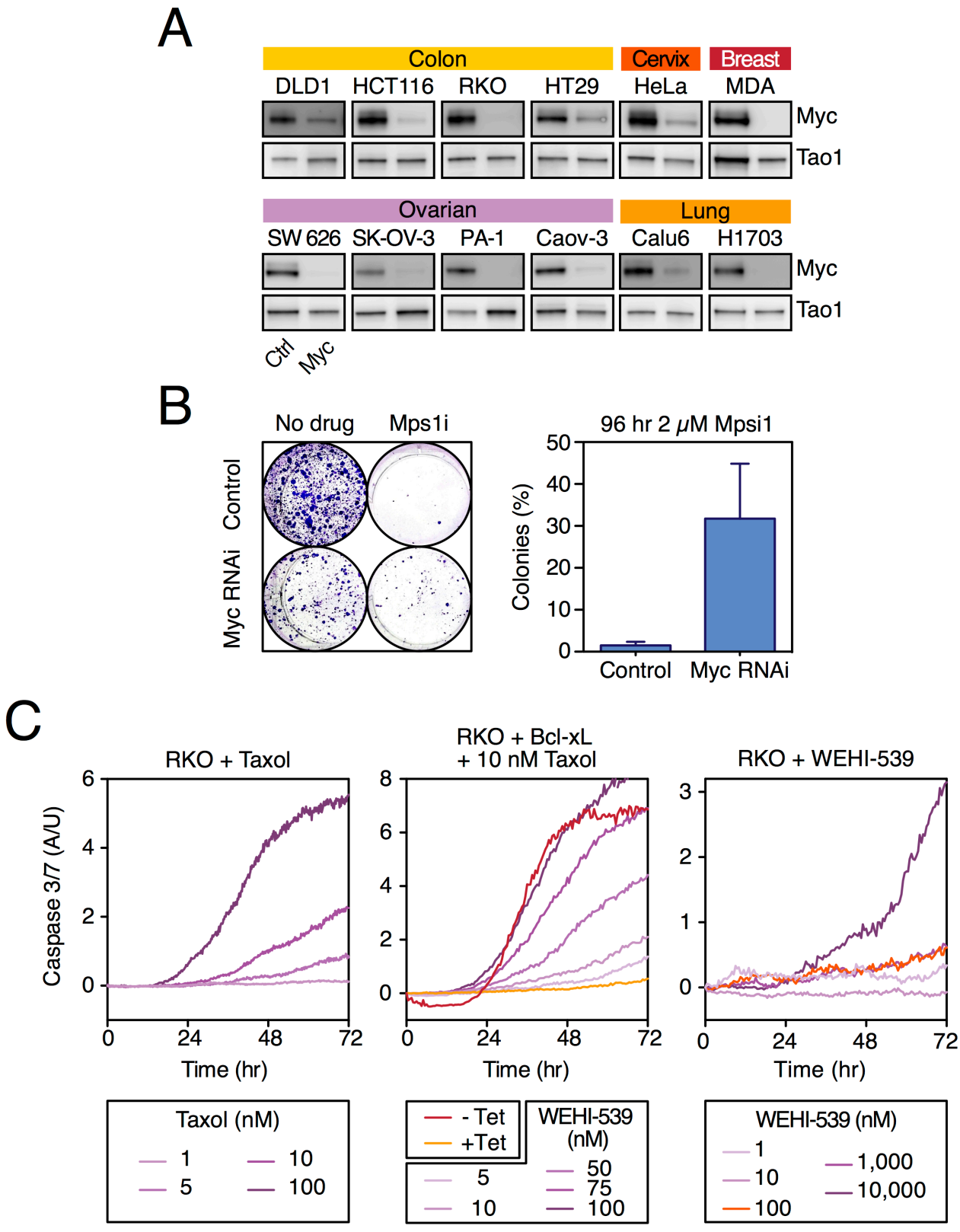

Figure S4, related to Figure 4. Myc promotes post-mitotic death. (**A**) Immunoblots showing RNAi-mediated inhibition of Myc in the panel of cell lines used in Fig. 4A. Each pair of lanes shows the non-targeting control on the left and the Myc siRNA on the right. (**B**) Colony formation assay of RKO cells 6 days following exposure to the Mps1 inhibitor AZ3146 for 96 hr. Values represent mean ± SEM from three independent experiments. (**C**) Caspase 3/7 assays showing apoptosis induction in RKO cells. Left panel shows a taxol titration. 10 nM was selected for the experiment in Fig. 4D. Middle panel shows that tet-induction of Bcl-xL blocks apoptosis in the presence of 10 nM taxol but that this is reverted by titrating in the Bcl-xL inhibitor WEHI-539. 100 nM was selected for the experiment in Fig. 4D. Right panel shows that in the absence of antimitotic agents, while 10 μM WEHI-539 induces apoptosis, 100 nM is relatively benign.

Table S4, related to Figure 4. Effect of c-Myc RNAi in response to 8 antimitotic agents in 12 cell lines from different tumour types.
Values represent IncuCyte-based Caspase 3/7 readings (AU) at 96 hrs used to generate Fig. 4A.

	Taxol		Nocodazole		Eg5i AZ138		Plk1i BI 2356		Cenp-Ei GSK923295		Aurora Ai MLN8054		Aurora Bi ZM447439		Mps1i AZ3146	
Cell Line	Ctrl	Myc	Ctrl	Myc	Ctrl	Myc	Ctrl	Myc	Ctrl	Myc	Ctrl	Myc	Ctrl	Myc	Ctrl	Myc
Calu6	510.0	389.5	498.5	338.0	355.5	259.5	479.5	407.0	555.0	350.0	391.5	296.5	464.5	271.5	492.0	177.0
Caov3	501.0	508.5	695.0	429.5	387.0	385.0	525.5	388.0	432.5	458.5	374.0	422.5	342.5	278.5	430.0	492.0
DLD-1	154.0	146.5	129.0	125.5	92.5	56.5	131.5	126.5	142.5	104.0	126.5	176.0	175.0	167.5	228.5	84.5
H1703	307.5	394.0	366.0	403.5	397.5	333.5	255.5	355.5	492.5	539.5	357.5	313.5	355.5	367.0	352.5	275.0
HCT116	367.5	145.5	381.5	127.5	247.5	150.0	289.5	120.0	344.0	119.0	253.0	61.0	175.5	31.0	552.0	223.0
HeLa	149.0	68.5	198.0	142.0	145.0	78.0	128.0	57.5	141.0	76.0	104.0	88.0	110.0	75.5	363.0	157.5
HT29	304.5	156.0	251.0	126.5	187.5	188.0	210.5	113.5	335.5	311.5	212.5	99.0	282.5	76.0	207.0	65.5
MDA	57.0	3.0	32.5	8.0	70.0	8.5	31.5	2.0	37.0	7.0	15.5	-1.0	35.5	1.5	27.5	6.5
PA1	70.0	51.8	37.1	19.6	59.5	30.1	51.8	38.5	70.0	17.5	64.4	23.8	78.4	33.6	61.6	16.8
RKO	452.5	329.5	567.0	205.0	402.0	201.0	272.0	32.0	311.5	272.5	194.5	44.0	143.0	36.0	521.5	45.5
SKOV3	150.5	77.0	65.0	31.0	75.5	57.5	117.5	58.5	83.5	45.0	25.0	12.0	29.0	8.0	37.5	10.5
SW262	20.0	15.5	13.5	9.5	16.0	9.0	20.0	9.0	20.5	10.0	14.0	10.5	13.5	10.5	15.5	10.0

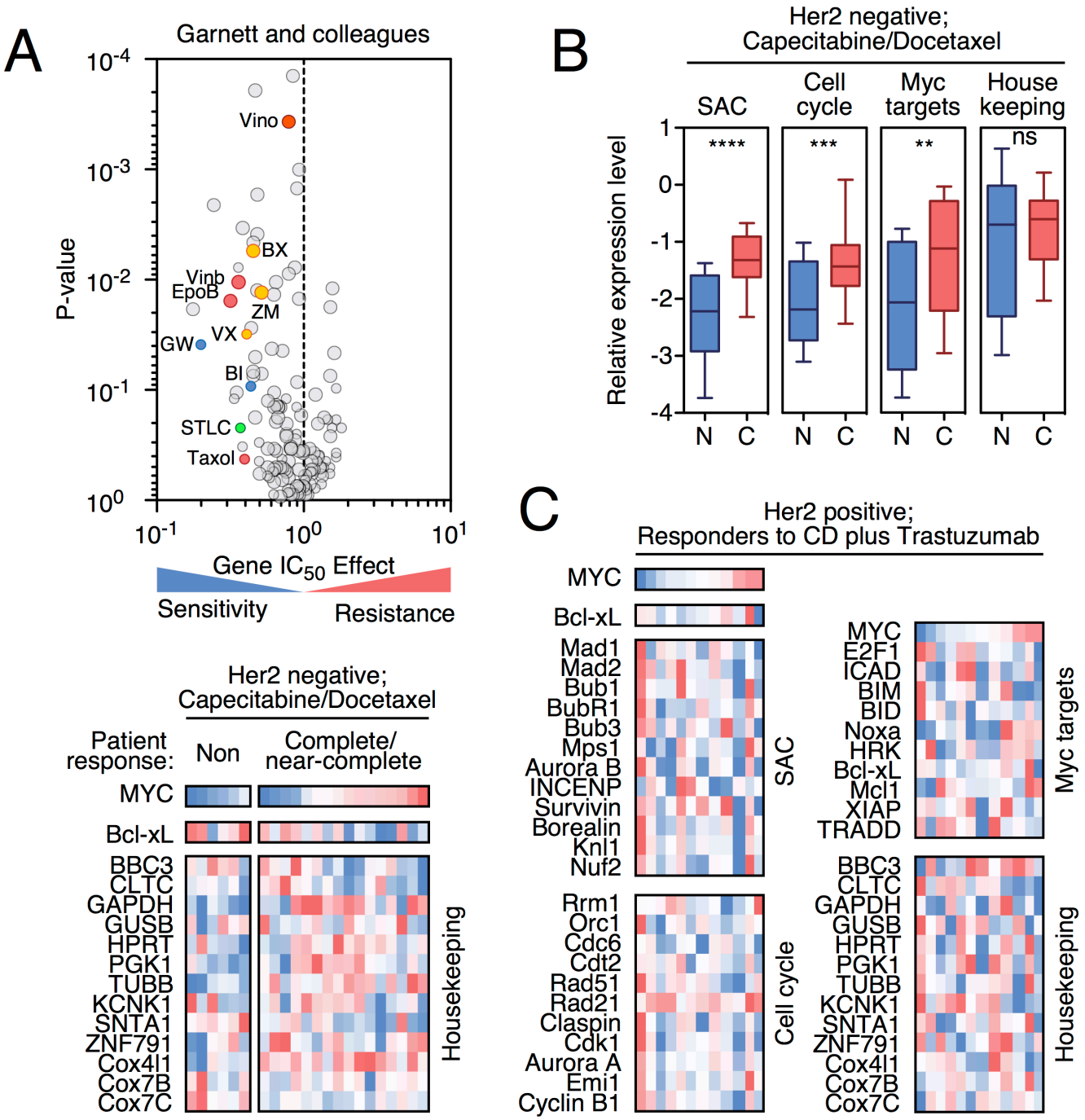

Figure S5, related to Figure 5. Overexpression of Myc sensitizes cancer cells to antimitotic agents. (**A**) Volcano plot showing the gene IC_{50} effect and significance (inverted) of *MYC*-drug associations. Each circle represents a single drug effect and the size is proportional to the number of Myc overexpressing cell lines screened (range 26-50). Primary data is derived from www.cancerrxgene.org (Garnett et al., 2012; Yang et al., 2013). Taxol, vinorelbine, vinblastine and epothilone B are microtubule inhibitors; BX-795, ZM447439, and VX-680 are Aurora kinase inhibitors; GW843682X and BI-2536 are Plk1 inhibitors; *S*-Trityl-L-cysteine is an Eg5/KSP inhibitor. (**B**) Box-and-whisker plots (median, interquartile and full range) showing the relative expression levels of SAC, cell cycle and Myc-regulated apoptosis clusters in tumours that either do not respond (N) or show complete/near-complete responses (C) to capecitabine and docetaxel chemotherapy. (**C**) Heat maps showing gene expression profiles of 12 Her2-positive tumours treated with capecitabine and docetaxel plus Trastuzumab (responders), indicating no obvious correlation with Myc. As in Fig. 5C, each column represents a patient sample and the colour code indicates the relative expression level of the genes indicated, with the sample with the highest value dark red and the lowest value dark blue. Also shown are the housekeeping controls genes to accompany the data in Fig. 5C. Primary data for (B) and (C) are derived from (Glück et al., 2012).

Table S5, related to Figure 5. Gene IC_{50} effect data for *MYC*. Used to generate Fig. 5B and S5A.
Source: www.cancerrxgene.org. Yang W, et al. Nucleic Acids Research (2013) 41; D955-61.

Drug	Drug Target	Effect	P-value	No. of mutations
Gemcitabine	DNA replication	0.199	0.020	47
GW843682X	PLK1	0.226	0.041	26
Thapsigargin	ER Ca^{2+} ATPase	0.266	0.002	47
Epothilone B	Microtubules	0.337	0.016	47
CMK	RSK	0.356	0.127	26
Obatoclax	BCL-2, BCL-XL, MCL-1	0.374	0.110	47
Vinblastine	Microtubules	0.387	0.011	50
BMS-536924	IGF1R	0.387	0.008	26
STLC	KIF11	0.396	0.233	26
Sunitinib	PDGFRA, PDGFRB, KDR, KIT, FLT3	0.404	0.355	26
Cisplatin	DNA crosslinker	0.406	0.003	50
Paclitaxel	Microtubules	0.414	0.457	26
VX-680	Aurora A/B/C, FLT3, ABL1, JAK2,	0.437	0.033	26
Etoposide	TOP2	0.456	0.029	47
BI-2536	PLK1/2/3	0.464	0.096	26
Cytarabine	DNA synthesis	0.467	0.072	50
QS11	ARFGAP	0.468	0.005	47
BX-795	TBK1, PDK1, IKK, AURKB/C	0.476	0.006	49
GSK-650394	SGK3	0.480	0.077	47
GDC-0449	SMO	0.484	0.000	50
GDC0941	PI3K (class 1)	0.485	0.054	49
Camptothecin	TOP1	0.493	0.191	50
AICAR	AMPK agonist	0.507	0.004	50
Vorinostat	HDAC inhibitor Class I, IIa, IIb, IV	0.507	0.013	50
TW 37	BCL-2, BCL-XL	0.510	0.002	49
Tipifarnib	Farnesyl-transferase (FNTA)	0.517	0.612	47
BMS-509744	ITK	0.521	0.314	26
NVP-TAE684	ALK	0.524	0.473	26
ZM-447439	AURKB	0.528	0.014	49
Mitomycin C	DNA crosslinker	0.538	0.076	47
BMS-754807	IGF1R	0.578	0.131	47
AZD6244	MEK1/2	0.579	0.371	49
Roscovitine	CDKs	0.583	0.631	27
ATRA	Retinoic acid receptor agonist	0.583	0.535	50
JW-7-52-1	MTOR	0.595	0.688	26
AZD-2281	PARP1/2	0.619	0.044	50
MS-275	HDAC	0.628	0.591	27
Doxorubicin	DNA intercalating	0.635	0.113	47
MG-132	Proteasome	0.637	0.949	27

Drug	Drug Target	Effect	P-value	No. of mutations
BAY 61-3606	SYK	0.638	0.364	47
Methotrexate	Dihydrofolate reductase (DHFR)	0.642	0.014	50
Axitinib	PDGFR, KIT, VEGFR	0.642	0.560	50
Pazopanib	VEGFR, PDGFRA, PDGFRB, KIT	0.644	0.735	47
OSU-03012	PDK1 (PDPK1)	0.648	0.150	47
Nilotinib	ABL	0.660	0.532	50
CEP-701	FLT3, JAK2, NTRK1, RET	0.663	0.206	50
AZD7762	CHK1/2	0.664	0.011	50
AS601245	JNK	0.665	0.381	47
OSI-906	IGF1R	0.669	0.143	47
PD-0325901	MEK1/2	0.674	0.153	49
AG-014699	PARP1, PARP2	0.687	0.151	49
Docetaxel	Microtubules	0.688	0.186	50
PD-0332991	CDK4/6	0.694	0.995	49
Bosutinib	SRC, ABL, TEC	0.706	0.538	50
CCT018159	HSP90	0.710	0.152	49
Elesclomol	HSP70	0.710	0.701	50
GSK-1904529A	IGF1R	0.717	0.047	47
Pyrimethamine	Dihydrofolate reductase (DHFR)	0.724	0.460	27
Bexarotene	Retinioic acid X family agonist	0.726	0.535	47
MK-2206	AKT1/2	0.733	0.555	49
Parthenolide	NFKB1	0.756	0.127	27
SB590885	BRAF	0.759	0.279	49
SB 216763	GSK3A/B	0.760	0.213	48
KU-55933	ATM	0.764	0.583	49
JNJ-26854165	MDM2	0.770	0.264	49
GSK269962A	ROCK	0.778	0.920	27
AZD6482	PI3Kb	0.783	0.894	47
CCT007093	PPM1D	0.783	0.474	49
Vinorelbine	Microtubules	0.784	0.000	47
LAQ824	HDAC	0.788	0.009	47
CI-1040	MEK1/2	0.795	0.683	50
NU-7441	DNAPK	0.810	0.967	49
GW 441756	NTRK1	0.817	0.370	50
AKT inhibitor VIII	AKT1/2	0.820	0.370	47
Lenalidomide	TNF alpha	0.823	0.354	50
AUY922	HSP90	0.833	0.000	47
IPA-3	PAK	0.838	0.957	47

ABT-263	BCL2, BCL-XL, BCL-W	0.853	0.303	49
RDEA119	MEK1/2	0.856	0.008	49
RO-3306	CDK1	0.881	0.794	49
VX-702	p38	0.885	0.812	50
Cyclopamine	SMO	0.886	0.269	27
Embelin	XIAP	0.886	0.002	47
A-443654	AKT1/2/3	0.894	0.154	26
JNK-9L	JNK	0.904	0.088	47
Bleomycin	DNA damage	0.905	0.001	47
AZD8055	mTORC1/2	0.909	0.376	49
KIN001-135	IKKE	0.914	0.956	27
PD-173074	FGFR1/3	0.917	0.943	49
PLX4720	BRAF	0.918	0.842	49
EHT 1864	Rac GTPases	0.923	0.574	49
Gefitinib	EGFR	0.924	0.847	50
NVP-BEZ235	PI3K (Class 1) and mTORC1/2	0.926	0.016	49
Nutlin-3a	MDM2	0.950	0.182	49
FH535	unknown	0.971	0.382	47
JNK Inhibitor VIII	JNK	0.975	0.392	49
SL 0101-1	RSK, AURKB, PIM3	0.975	0.814	49
WH-4-023	SRC family, ABL	0.986	0.709	26
Bicalutamide	Androgen receptor (ANDR)	0.990	0.958	47
ABT-888	PARP1/2	0.995	0.837	50
TGX221	PI3K beta	0.999	0.815	27
PF-4708671	p70 S6KA	1.000	0.637	49
Salubrinal	GADD34-PP1C phosphatase	1.030	0.884	27
NSC-87877	SHP1/2 (PTN6/11)	1.050	0.937	47
PF-562271	FAK	1.060	0.368	47
BIRB 0796	p38, JNK2	1.080	0.763	49
Bortezomib	Proteasome	1.090	0.594	27
Bryostatin 1	PRKC	1.090	0.556	47
681640	WEE1, CHK1	1.090	0.472	49

AMG-706	VEGFR, RET, c-KIT, PDGFR	1.110	0.606	49
FTI-277	Farnesyl transferase (FNTA)	1.130	0.566	47
Shikonin	unknown	1.140	0.395	47
CGP-60474	CDK1/2/5/7/9	1.150	0.855	26
Temsirolimus	MTOR	1.170	0.116	50
Lapatinib	EGFR, ERBB2	1.190	0.465	27
CHIR-99021	GSK3B	1.190	0.216	47
BMS-708163	gamma-secretase	1.200	0.432	49
Midostaurin	KIT	1.230	0.545	47
Erlotinib	EGFR	1.240	0.424	23
AZD-0530	SRC, ABL1	1.250	0.764	26
CGP-082996	CDK4	1.260	0.534	26
PAC-1	CASP3 activator	1.260	0.643	47
AZ628	BRAF	1.280	0.610	27
Rapamycin	MTOR	1.300	0.546	26
LFM-A13	BTK	1.310	0.191	47
PF-02341066	MET, ALK	1.360	0.469	26
XMD8-85	ERK5 (MK07)	1.390	0.200	27
17-AAG	HSP90	1.420	0.078	49
A-770041	SRC family	1.430	0.629	26
WZ-1-84	BMX	1.440	0.542	26
DMOG	Prolyl-4-Hydroxylase	1.440	0.018	47
AP-24534	ABL	1.440	0.283	47
AZD6482	PI3Kb (P3C2B)	1.470	0.012	47
Imatinib	ABL, KIT, PDGFR	1.490	0.240	26
BIBW2992	EGFR, ERBB2	1.510	0.048	50
Z-LLNle-CHO	g-secretase	1.560	0.103	26
PHA-665752	MET	1.570	0.196	26
GNF-2	BCR-ABL	1.580	0.405	26
Dasatinib	ABL, SRC, KIT, PDGFR	1.580	0.440	26
Sorafenib	PDGFRA, PDGFRB, KDR, KIT, FLT3	1.690	0.234	27

Notes: The volcano plot (Fig. S5A) visualises the correlation of drug sensitivity data with genetic events calculated using a multivariate ANOVA. Gene specific volcano plots represent the effect of a mutated gene (e.g. BRAF) on the responses to all drugs analysed. The volcano plot presents three pieces of data:

• x-axis: The magnitude of the effect that genetic events have on cell lines IC_{50} values in response to a drug. IC_{50} values were correlated with the status of commonly altered cancer genes using a two way multivariate ANOVA, with mutation status and tissue type as factors. The effect size is proportional to the difference in mean IC_{50} between wild-type and mutant cell lines. Numbers less than 1 indicate drug sensitivity, numbers greater than 1 indicate drug resistance.

• y-axis: The p-value from the MANOVA of a drug-gene interaction on an inverted log10 scale.

• Size of each circle: The number of genetic events contributing to the analysis for a given gene or drug.

(See www.cancerrxgene.org for more details.)

Table S6, related to Figure 5. Gene expression profiles and patient responses to Capecitabine/Docetaxel chemotherapy. Used to generate Fig. 5C and S5C. **Source:** www.oncomine.org. Glück et al (2012) Breast Cancer Res Treat. 132(3):781-91.

Sample Number	35	34	37	33	32	36	124	113	117	125	123	114	110	119	118	122	112	111	116	115	121	120
Response[1]	N	N	N	N	N	N	CR	NC	CR	CR	CR	NC	NC	CR	CR	CR	NC	NC	CR	NC	CR	CR
Aurora A	-2.66	-1.56	-2.51	-2.76	-3.17	-3.25	-3.06	-2.12	-3.62	-0.45	-1.72	-2.34	-1.78	-1.86	-1.57	-1.37	-1.32	-0.79	-1.68	-2.82	-1.23	-0.40
Aurora B	-2.31	-1.71	-1.94	-2.00	-2.12	-1.56	-2.01	-1.64	-2.07	-1.90	-1.69	-2.07	-1.74	-1.66	-1.18	-0.85	-0.62	-0.95	-2.03	-2.46	-0.78	-0.64
BBC3	0.09	-0.06	0.34	0.13	0.18	-0.23	0.26	0.06	-0.03	0.45	0.03	0.10	-0.26	-0.04	-0.39	-0.31	0.04	0.00	0.15	-0.18	-0.16	-0.41
Bcl-xL	0.18	0.10	-0.62	-0.24	-0.14	0.25	-0.05	-0.35	0.04	-0.09	-0.37	-0.15	-0.49	-0.14	-0.69	-0.33	-0.46	-0.74	-0.71	0.05	-0.63	-0.39
Bid	-0.43	0.43	-0.91	-0.51	-0.92	-1.19	0.13	-0.01	-1.49	-0.54	0.22	-0.27	0.27	0.88	0.74	0.92	0.53	-0.10	-0.04	-0.49	0.18	0.34
Bim	-0.45	-0.43	-0.39	-0.84	-0.94	-0.80	-0.90	-0.63	-0.67	-0.66	-0.17	-0.42	-0.29	-0.03	-0.53	-0.14	-0.66	0.62	-0.85	-0.73	-0.14	0.50
Borealin	-2.63	-1.38	-2.31	-2.11	-2.69	-3.19	-2.54	-1.09	-3.30	-0.76	-0.49	-1.99	-1.42	-1.55	-0.47	-1.33	-1.13	-1.25	-1.38	-2.44	-0.41	0.32
Bub1	-3.37	-1.81	-3.76	-3.17	-3.70	-4.66	-3.69	-2.27	-5.04	-3.03	-1.91	-2.48	-1.95	-1.84	-1.18	-1.39	-2.08	-1.23	-2.33	-3.86	-1.99	-0.85
Bub3	-2.09	-1.52	-0.90	-0.62	-1.42	-2.17	-1.22	-1.23	-1.11	-0.27	0.04	-0.84	-1.38	-0.75	-0.91	-0.73	-1.33	1.03	-1.03	-1.46	0.39	-0.48
BubR1	-1.64	-1.07	-3.36	-1.78	-2.39	-2.07	-2.26	-2.15	-1.97	-2.30	-1.93	-1.47	-1.07	-1.85	-1.44	-1.33	-1.40	-1.93	-1.72	-2.11	-0.93	-0.37
Cdc6	-2.57	-2.71	-3.03	-2.98	-2.87	-3.77	-3.68	-2.76	-3.75	0.29	-1.52	-2.85	-1.39	-1.55	-1.86	-2.18	-1.68	-1.82	-2.76	-3.65	-2.24	-1.36
CDK1	-3.30	-2.18	-2.64	-2.54	-3.81	-4.14	-2.66	-1.99	-4.35	-1.46	-1.75	-1.69	-1.64	-0.78	-0.50	-0.14	-1.24	-0.67	-1.11	-3.10	-0.81	-1.00
Cdt2	-1.50	0.63	-1.32	-2.01	-2.61	-3.22	-2.51	-1.81	-3.41	-1.39	-0.83	-1.99	-2.05	-1.17	-0.99	0.04	-0.88	0.07	-0.96	-2.06	-2.17	-0.69
Claspin	-0.93	-0.42	-1.20	-0.90	-1.36	-1.28	-1.23	-1.02	-2.10	-0.21	-0.89	-0.84	-0.60	0.09	-1.05	-0.67	-1.49	0.16	-1.20	-1.48	-0.02	-0.10
CLTC	-0.51	-0.23	-0.34	-0.57	-0.33	-0.82	0.00	0.50	2.79	-0.07	-0.33	-0.61	-0.26	-0.67	-0.85	-0.70	-0.35	1.49	-0.68	-0.77	-0.60	-0.91
Cox4l1	-1.68	-2.14	-0.47	-0.79	-1.00	-0.92	-0.12	-0.45	-0.48	-0.12	-0.58	-0.22	-0.99	-0.03	-0.38	0.24	0.27	-0.04	-0.33	-0.85	0.09	-0.54
Cox7B	0.35	2.24	-0.54	-0.15	-0.86	0.55	-0.18	-0.73	-0.70	0.79	0.12	-0.50	-0.01	0.75	-0.03	0.35	-1.69	0.37	-0.08	0.06	0.36	-0.06
Cox7C	1.30	2.10	-0.07	0.08	-0.16	0.99	-0.26	-0.68	0.03	0.04	-0.34	-0.19	-0.91	-0.58	-0.53	-0.06	-0.88	0.24	-0.40	0.36	-0.24	-0.43
E2F1	-1.46	-0.75	-1.92	-2.06	-2.63	-2.43	-1.84	-0.97	-2.53	-1.08	0.18	-1.44	-0.95	0.11	-0.14	-0.25	-1.29	-0.52	-0.20	-1.58	-1.18	-0.03
Emi1	-2.42	-2.19	-2.48	-1.58	-2.05	-3.31	-2.21	-1.99	-2.99	-1.69	-0.73	-1.28	-0.72	-1.29	-1.36	-1.12	-1.64	-1.51	-1.58	-2.62	-0.41	0.13
GAPDH	-1.94	-2.58	-1.69	-1.94	-2.39	-2.58	-1.87	-1.88	-2.41	-0.78	-0.49	-0.50	-1.20	-0.97	-0.68	-0.90	-1.50	-2.07	-1.30	-2.45	-0.56	-0.95
GUSB	0.35	-0.58	-0.14	0.54	0.17	0.33	0.73	-0.17	0.07	-0.03	0.19	0.35	-0.08	-0.22	0.52	0.16	0.02	0.17	0.11	0.81	-0.17	-0.33
HPRT	-1.42	0.33	-1.26	-1.58	-1.65	-2.85	-1.20	-1.89	-1.86	-0.24	-0.10	-0.66	-0.99	0.79	-0.54	-0.11	-0.60	-0.27	-0.64	-1.78	-1.06	-0.55
HRK	-0.34	-0.34	0.01	-0.67	-0.42	-0.74	0.20	-0.03	-0.84	0.23	1.74	0.78	0.53	0.32	-0.41	-0.04	-0.21	-0.26	-0.46	-0.14	0.93	0.46
ICAD	-1.10	-1.17	-0.97	-0.57	-0.91	-1.46	-0.80	-0.71	-1.59	-1.19	-0.49	-0.70	-1.17	-0.11	-0.04	0.14	-0.26	-0.92	-0.24	-0.95	-0.06	0.54
INCENP	-1.27	0.26	-2.58	-1.39	-1.87	-2.03	-1.55	-0.08	-2.86	-1.25	0.38	-0.94	-1.08	-1.16	-0.58	0.78	0.60	-0.69	0.00	-1.19	-0.33	-0.75
KCNK1	3.02	0.24	2.71	-1.12	-0.64	-0.75	0.34	1.37	-2.02	1.09	2.41	1.44	1.21	1.46	1.26	1.91	-0.70	-2.22	-0.23	0.36	0.91	-1.94
Knl1	-2.21	-0.82	-2.01	-1.96	-1.98	-2.57	-2.61	-1.76	-2.96	-1.65	-1.33	-1.71	-1.43	-1.37	-1.84	-0.63	-1.22	-0.73	-1.32	-2.40	-1.02	-0.97
Mad1	-1.79	-1.62	-1.13	-0.87	-1.19	-1.63	-0.87	-0.87	-1.03	-0.47	-0.87	-0.85	-1.30	-0.49	-1.04	-0.89	-0.13	0.39	-1.14	-1.58	-1.12	-0.86
Mad2	-5.03	-3.59	-2.95	-2.26	-3.09	-5.54	-2.94	-2.69	-4.16	-1.54	-1.55	-1.62	-1.82	-1.37	-1.25	-1.11	-0.68	-0.75	-0.94	-3.89	-0.79	-0.72
Mcl1	-0.66	-1.25	0.02	0.15	-0.29	-0.48	0.10	1.09	-0.69	0.34	0.95	0.00	1.23	0.56	0.81	0.03	0.63	0.39	0.66	-0.16	0.41	1.34
Mps1	-2.54	-1.86	-3.28	-2.11	-2.79	-3.60	-3.22	-2.21	-3.74	-1.48	-0.57	-1.59	-0.90	-1.20	-0.28	-0.27	-0.15	-0.15	-1.14	-3.36	-1.12	0.35
MYC	-3.20	-3.11	-2.91	-2.78	-2.55	-2.17	-3.18	-3.07	-2.96	-2.84	-2.24	-1.91	-1.91	-1.67	-1.20	-1.05	-1.02	-0.88	-0.77	-0.51	0.38	1.37
Noxa	-1.98	-2.25	-2.68	-2.01	-0.28	-3.69	-1.47	-3.40	-4.13	-1.71	-0.66	-2.26	-1.74	-3.29	-1.67	-4.12	-1.52	-1.18	-2.31	-2.55	-2.25	-0.38
Nuf2	-3.17	-1.50	-2.44	-2.73	-3.27	-3.97	-2.60	-1.31	-3.50	-2.76	-0.72	-1.43	-0.67	-1.36	-0.16	-0.63	-0.41	-0.49	-0.66	-2.71	-0.45	1.24
Orc1	-1.80	-2.44	-2.39	-2.15	-2.18	-1.35	-1.96	-2.44	-2.71	-1.97	-0.57	-2.15	-1.46	-1.32	-1.93	-2.02	-0.90	-2.49	-2.78	-1.99	-1.02	-1.27
PGK1	-1.34	-1.87	-2.22	-2.04	-2.44	-2.24	-1.57	-1.90	-2.56	-1.09	-1.00	-0.19	-1.15	-1.06	-1.11	-0.65	-1.58	-1.69	-1.78	-2.10	-1.39	-1.96

Sample Number	35	34	37	33	32	36	124	113	117	125	123	114	110	119	118	122	112	111	116	115	121	120
Response[1]	N	N	N	N	N	N	CR	NC	CR	CR	CR	NC	NC	CR	CR	CR	NC	NC	CR	NC	CR	CR
Rad21	-1.71	-1.38	-0.77	-0.58	-0.26	-1.66	0.16	0.05	1.35	-1.09	0.25	-0.16	-0.97	-0.03	-0.11	-0.20	0.52	0.37	0.80	-0.43	0.46	0.47
Rad51	-2.31	-0.92	-2.56	-2.00	-2.89	-3.25	-2.32	-1.81	-3.47	-1.53	-0.78	-2.36	-0.66	-1.16	-0.99	-0.49	-0.32	-0.52	-1.42	-2.61	-1.86	-0.46
Rrm1	-2.18	-1.52	-0.97	-0.61	-1.38	-1.98	-1.82	-1.23	-1.83	-1.29	-1.07	-1.76	-0.62	-1.82	-0.56	-0.77	-0.47	-0.77	-1.74	-1.19	-0.84	-0.52
SNTA1	-0.14	-0.04	0.05	-0.14	-0.01	0.61	-0.20	-0.25	0.00	0.13	-0.46	0.04	-0.09	-0.55	-0.50	-0.34	-0.45	-0.81	-0.60	0.47	-0.61	-0.73
Survivin	-3.17	-1.57	-3.14	-1.96	-3.47	-4.38	-3.12	-1.11	-3.49	-1.33	-1.37	-0.85	-1.78	-1.45	-0.97	-1.35	0.92	0.51	-2.18	-2.58	1.20	-0.94
TRADD	-2.44	-2.37	-0.77	-0.90	-0.90	-2.29	-0.25	0.00	-0.89	-0.38	-0.04	-0.62	-0.47	-0.17	-0.47	-0.55	1.11	-0.65	-0.52	-1.55	-0.47	-0.15
TUBB	-2.50	-2.45	-1.53	-1.35	-1.39	-2.07	-1.18	-0.41	-1.77	-1.09	-1.30	-1.35	-0.77	-1.07	-0.44	-0.68	-0.73	-1.73	-0.63	-1.72	0.00	-0.47
XIAP	0.60	-0.45	1.89	-0.75	0.23	0.27	0.02	-0.33	0.33	1.26	0.72	0.91	0.48	1.34	0.00	0.35	-1.28	0.93	0.86	-0.32	0.33	0.11
ZNF791	-0.93	-1.06	0.00	0.05	0.35	-0.55	-0.27	0.60	0.65	-0.05	-0.16	-0.63	0.15	0.35	-0.21	-0.30	-0.07	-0.96	0.07	-0.01	0.38	0.48

Values represent Log2 median-centered ratio.

[1] Patient treatment response: N, no response; NC, near complete response; CR, complete response.

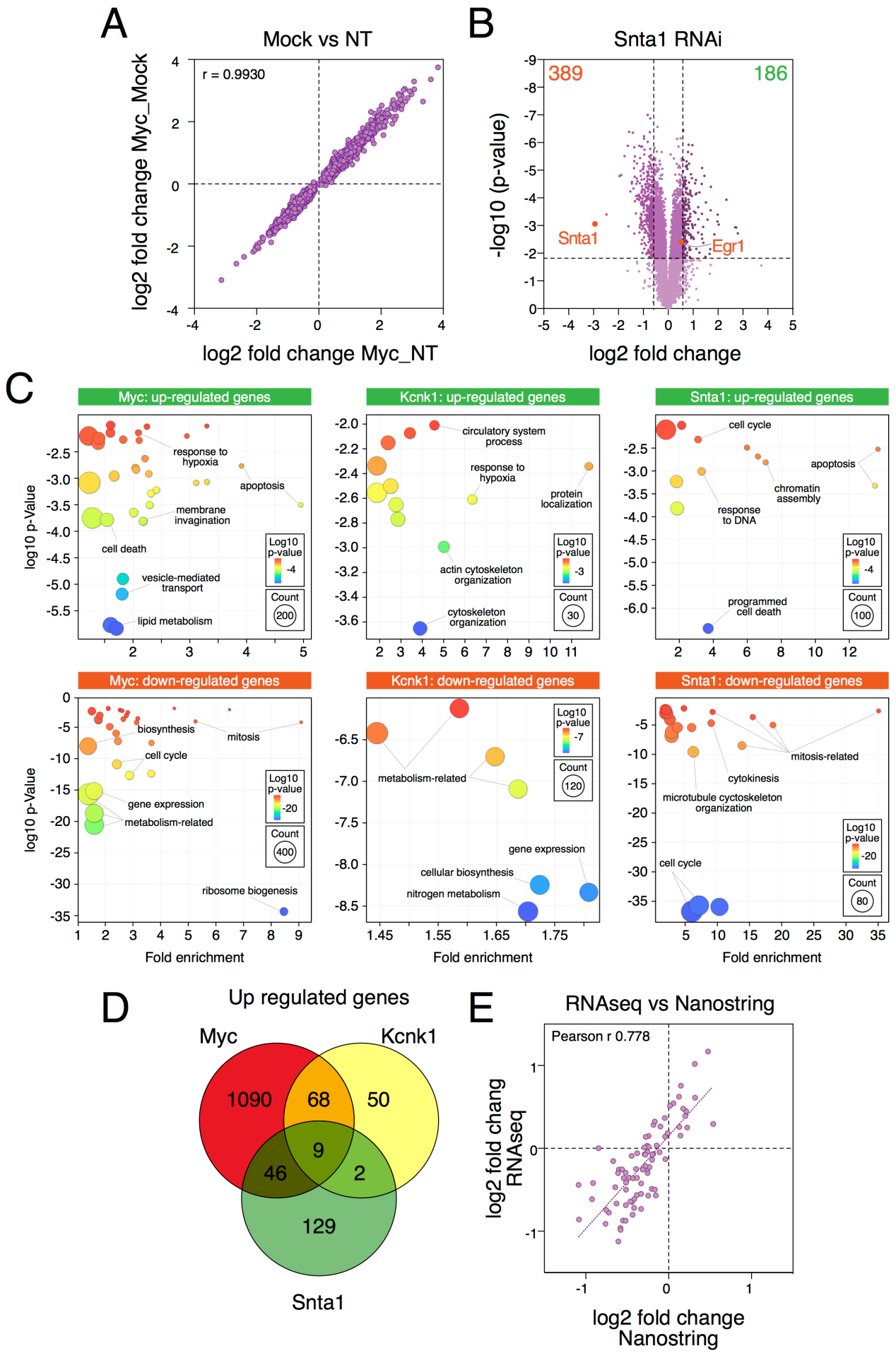
A
Mock vs NT
r = 0.9930
log2 fold change Myc_Mock
log2 fold change Myc_NT
B
Snta1 RNAi
389
186
Snta1
Egr1
-log10 (p-value)
log2 fold change
C
Myc: up-regulated genes
response to hypoxia
apoptosis
membrane invagination
cell death
vesicle-mediated transport
lipid metabolism
Kcnk1: up-regulated genes
circulatory system process
response to hypoxia
protein localization
actin cytoskeleton organization
cytoskeleton organization
Snta1: up-regulated genes
cell cycle
apoptosis
chromatin assembly
response to DNA
programmed cell death
Myc: down-regulated genes
biosynthesis
mitosis
cell cycle
gene expression
metabolism-related
ribosome biogenesis
Kcnk1: down-regulated genes
metabolism-related
gene expression
cellular biosynthesis
nitrogen metabolism
Snta1: down-regulated genes
mitosis-related
cytokinesis
microtubule cytoskeleton organization
cell cycle
log10 p-Value
Fold enrichment
Log10 p-value
Count
D
Up regulated genes
Myc
Kcnk1
Snta1
1090
68
50
9
46
2
129
E
RNAseq vs Nanostring
Pearson r 0.778
log2 fold chang RNAseq
log2 fold change Nanostring

Figure S6, related to Figure 7. Global gene expression profiling. (**A**) Gene expression fold changes following Myc RNAi, normalized to either mock transfected (*y*-axis) or cells transfected with a non-targeting control siRNA (*x*-axis). Each value is the average derived from five biological replicates for mock and four each for the non-targeting control and Myc siRNA. Because of the excellent correlation, all subsequent analysis was performed with values normalized to the non-targeting control siRNA. (**B**) Volcano plot showing the gene expression changes induced by transfection of *SNTA1* siRNA #4. (**C**) Gene ontology analysis of the up and downregulated genes following transfection of siRNAs targeting Myc, Kcnk1 and Snta1. Gene Ontology analysis was performed with DAVID Bioinformatics Resources 6.7 (Huang da et al., 2009) then visualized with Revigo (Supek et al., 2011). The Snta1 siRNA deregulated 575 genes, with *SNTA1* itself the most repressed gene. Cell cycle and mitosis-related gene ontology terms feature heavily, consistent with this siRNA accelerating mitotic exit. Interestingly, FoxM1, which drives G2/M gene expression was reduced 1.75-fold (not shown), indicating that this siRNA may disrupt mitotic controls by deregulating FoxM1 (Laoukili et al., 2005). (**D**) Venn diagram showing the number of common upregulated genes. (**E**) Fold changes for the genes analyzed in Fig. 3A showing good correlation between the Nanostring and RNAseq-based measurements.

Table S7, related to Figure 7. RNA-Seq-derived gene expression analysis. Used to generate Fig. 7A and S6B. (Provided as an Excel file).

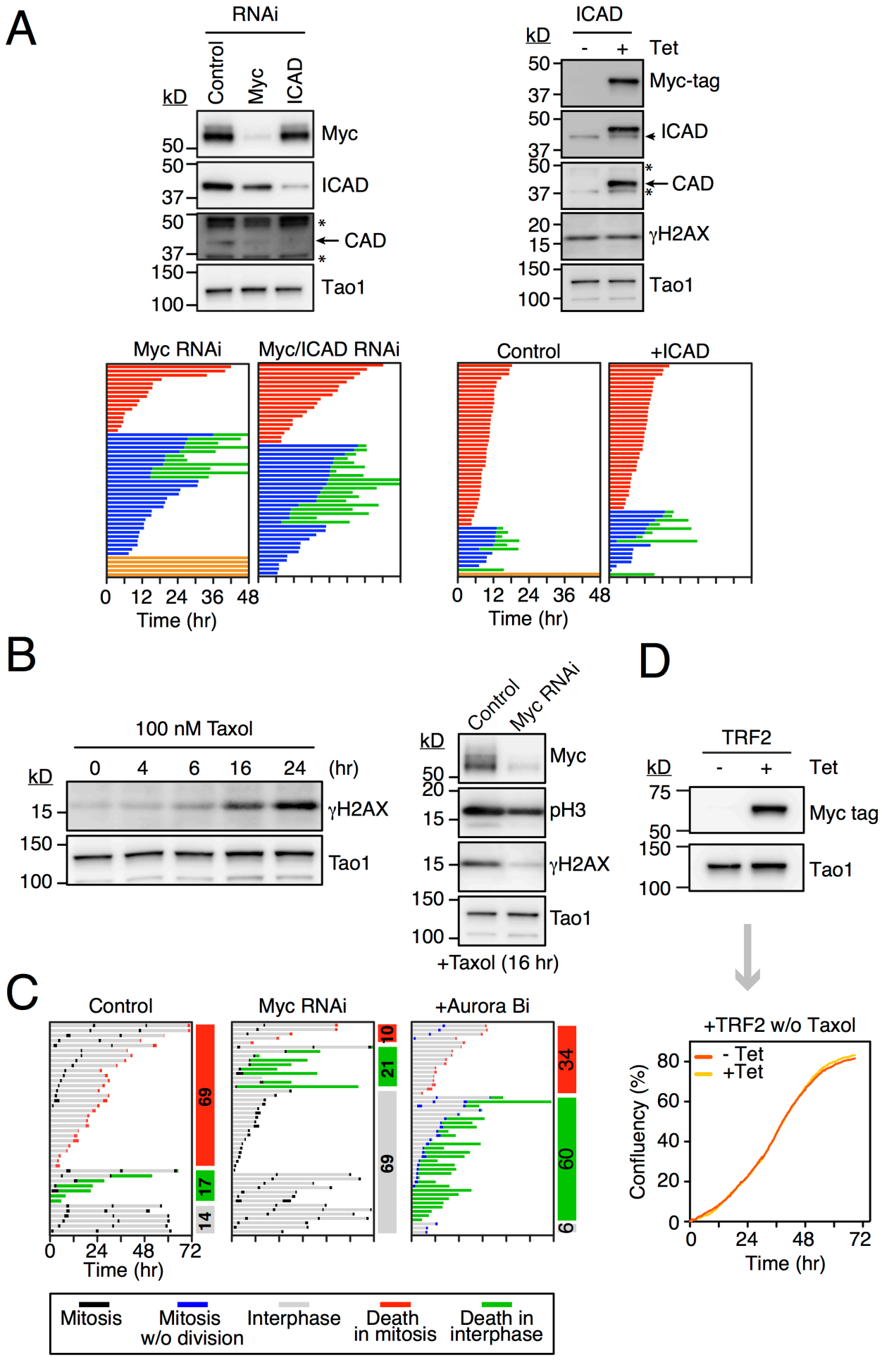
A
RNAi
Control
Myc
ICAD
kD
Myc
ICAD
CAD
Tao1
ICAD
Tet
Myc-tag
γH2AX
Myc RNAi
Myc/ICAD RNAi
Control
+ICAD
Time (hr)
B
100 nM Taxol
(hr)
γH2AX
Tao1
Control
Myc RNAi
pH3
+Taxol (16 hr)
C
Control
Myc RNAi
+Aurora Bi
Time (hr)
Mitosis
Mitosis w/o division
Interphase
Death in mitosis
Death in interphase
D
TRF2
Myc tag
+TRF2 w/o Taxol
- Tet
+Tet
Confluency (%)

Figure S7, related to Figure 8. Inhibition of ICAD/CAD and telomere deprotection enhances slippage. (**A**) Characterisation of ICAD RNAi and overexpression. Immunoblots show that inhibition of either Myc or ICAD reduces CAD levels. Fate profiles show that RNAi-mediated inhibition of ICAD in Myc RNAi cells does not further suppress DiM. Tet-induced overexpression of ICAD elevates levels of CAD but this has no obvious effect on DNA damage or DiM. Asterisks mark non-specific bands. (**B**) Immunoblot shows that taxol exposure induces γH2AX, indicating DNA damage, and that this is suppressed by Myc RNAi. (**C**) Fate profiles of RKO cells in the absence of taxol following RNAi-mediated co-repression of Bcl-xL and Mcl1. In contrast to fate profiles of taxol-treated cells, here, zero hr represents when imaging started as opposed to when the cell first entered mitosis. 69% of Bcl-xL/Mcl1-deficient cells undergo DiM, indicating that in the absence of pro-survival function, mitosis is a significant stress, inducing apoptosis without the addition of taxol. Co-repression of Myc reduces DiM in Bcl-xL/Mcl1-deficient cells to 10%, consistent with Myc counterbalancing pro-survival function. Exposing Bcl-xL/Mcl1-deficient cells to 2 μM ZM447439, a selective Aurora B inhibitor (Ditchfield et al., 2003), also reduces DiM in the absence taxol, to 34%. Note that Aurora B promotes telomere deprotection upon mitotic entry, activating a DNA damage signal (Hayashi et al., 2012). (**D**) Characterisation of a tet-inducible RKO cell line overexpressing the shelterin component TRF2, tagged with an N-terminal Myc epitope. Immunoblot shows induction of TRF2 with 1 μg/ml tetracycline and growth curves shows that, in the absence of taxol, this does not inhibit proliferation.

Supplemental Experimental Procedures

Cell lines

Colon carcinoma lines (RKO, DLD-1, HCT116, HT29), lung carcinoma lines (Calu6 and H1703) breast (MDA-MB-231) and ovarian cancer lines (SKOV3, PA1, SW626, Caov3) were obtained from the American Type Culture Collection. HeLa cells were as described (Taylor and McKeon, 1997), HCT116 $p53^{-/-}$ were provided by Bert Vogelstein (Bunz et al., 1998). Cells were cultured in DMEM plus 10% fetal calf serum (LifeTechnologies), 2 mM glutamine, 100 U/ml penicillin, and 100 U/ml streptomycin (Lonza). For PA1, SW626 and SKOV3, DMEM was replaced by Minimum Essential Media, Leibovitz's L-15 (Sigma-Aldrich) and McCoys (modified) 5A medium (Life Technologies) respectively. All lines were grown at 37°C in a humidified 5% CO_2 incubator. For the tertiary screen, we use an RKO line expressing a GFP-tagged histone H2B (Gascoigne and Taylor, 2008) so that mitotic index could be approximated by measuring the granularity of the chromatin.

siRNA sequences

The sequences of siRNAs used in this study are listed below. All siRNAs were from Dharmacon unless stated otherwise.

Target		siRNA sequence	Notes
Bcl-2		GGGAGAACAGGGUACGAUA GAAGUACAUCCAUUAUAAG GGAGGAUUGUGGCCUUCUU UCGCCGAGAUGUCCAGCCA	
Bcl-xL		GGACAGCAUAUCAGAGCUU GAAAUGACCAGACACUGAC CCUACAAGCUUUCCCAGAA UUAGUGAUGUGGAAGAGAA	
Bid		GGGAUGGACUGAACGGACA CUAGAGACAUGGAGAAGGA GCACCUACGUGAGGAGCUU GUAACUAACUGCAUACACU	
Bim		UGACCGAGAAGGUAGACAA CAACCACUAUCUCAGUGCA	Life Technologies
BubR1		AACGGGCAUUUGAAUAUGAAA	Positive control siRNA in library screen. (Ditchfield et al., 2003)
Egr1		GAUGAACGCAAGAGGCAUA CGACAGCAGUCCCAUUUAC GGACAUGACAGCAACCUUU GACCUGAAGGCCCUCAAUA	
Myc	#4 #5 #6 #8	CGAUGUUGUUUCUGUGGAA AACGUUAGCUUCACCAACA GGAACUAUGACCUCGACUA CUACCAGGCUGCGCGCAAA	These four siRNAs were pooled for routine use while #4 was used in isolation for the RNAi-rescue experiment (Fig. S2B).
G1		si*GLO* RISC-free siRNA (D-001600-01-05)	Additional negative control siRNA (Fig. S2A).
GAPDH (GA)		UGGUUUACAUGUUCCAAUA	Negative control siRNA in library screen.
Hrk		GGGAAGCCCUUUGGAAAUC GAUCGUAGAAACACAGAAU UCAAGGCGCUAGGCGACGA AGGCGGAACUUGUAGGAAC	
ICAD		GGCGAGAUCCGGACUCUAA GACAUUCUGGCCAUUGAUA ACGCAGAGCUUGCAUUCUC GAAAGAAGAUCUGUCCAGC	

KCNK1	#6	CGGUGGAGCUGCCCUAUGA	Active siRNA (Fig. S1)
Mcl1		CGAAGGAAGUAUCGAAUUU GAUUAUCUCUCGGUACCUU GAAGGUGGCAUCAGGAAUG GGUUUGGCAUAUCUAAUAA	
Non-targeting (NT)		UGGUUUACAUGUCGACUAA UGGUUUACAUGUUGUGUGA UGGUUUACAUGUUUUCUGA UGGUUUACAUGUUUUCCUA	Routine negative control siRNA pool.
Noxa		AAACUGAACUUCCGGCAGA GAACCUGACUGCAUCAAAA AAUCUGAUAUCCAAACUCU GCAAGAACGCUCAACCGAG	
Scramble (SC)		AAAACCAUCAUACCAGAGACA	Additional negative control siRNA (Fig. S2A).
SNTA1	#4	CAGAUUGGCUGGCUAACUG	Active siRNA (Fig. S1D)
Tao1 (T1)		GUAAUAUGGUCCUUUCUAA	Additional negative control siRNA (Fig. S2A). (Westhorpe et al., 2010)
XIAP		GUAGAUAGAUGGCAAUAUG GAACUGGGCAGGUUGUAGA GAAAGAGAUUAGUACUGAA GGACUCUACUACACAGGUA	
ZNF791	#1	GGGAAGACCCGAAUGUUGA	Active siRNA (Fig. S1D)

cDNAs

Open reading frames were generated either by using SuperScript One-Step RT-PCR with mRNA prepared from HeLa or RKO cells, or PCR amplified using Pfu Turbo with a plasmid as the template, then cloned into a pcDNA5/FRT/TO-based vector modified to include an N-terminal Myc or GFP epitope tag (Girdler et al., 2006). Myc and Omomyc were engineered with a C-terminal GFP tag, XIAP, Bcl-xL, ICAD and TRF2 were tagged with a Myc epitope at the N-terminus, and Bim was untagged. All ORFs were verified by sequencing.

Name	Accession	PCR primers (5' - 3')	Source
Bcl-xL	NM_138578.1	TCTCAGAGCAACCGGGAGCTG TCATTTCCGACTGAAGAGTGAG	RT-PCR
Bim	NM_138621.4	ATGGCAAAGCAACCTTCTG TCAATGCATTCTCCACACC	Thermo Scientific Clone ID 5213713
Myc	NM_002467.4	ATGCCCCTCAACGTTAGCTTC CGCACAAGAGTTCCGTAG	RT-PCR
ICAD	NM_004401.2	GAGGTGACCGGGGACGCCGGG CTATGTGGGATCCTGTCTGGC	RT-PCR
TRF2	NM_005652	GCGGGAGGAGGCGGGAGTAGC TCAGTTCATGCCAAGTC	Addgene 16066 (Karlseder et al., 2002)
XIAP	NM_001167.3	ACTTTTAACAGTTTTGAAGG TTAAGACATAAAAATTTTTTGCTTG	RT-PCR
Omomyc		ATGGAGGAGAATGTCAAG CGCACAAGAGTTCCGTAG GTTGCGGAAACAAAACGAACAGTTGA TCAACTGTTCGTTTTGTTTCCGCAAC CAAGCAGAGACGCAAAAGCTCATTTCTGA -AATCGACTTGTTG CAACAAGTCGATTTCAGAAATGAGCTTTT- GCGTCTC	(Soucek et al., 1998)

Antibodies

Primary antibodies for immunoblotting are listed below.

Antigen	Antibody name	Source/ Citation
Bcl-xL	Rabbit anti-Bcl-xL	Cell Signaling Technology
Bcl2	Mouse anti-Bcl2	BD Biosciences
Bid	Rabbit anti-Bid (Human specific)	Cell Signaling
Bim	Rabbit anti-Bim	BD Biosciences
Bub3	Sheep anti-Bub3	Holland and Taylor, unpublished
BubR1	Sheep anti-BubR1 (SBR1.1)	(Taylor et al., 2001)
Caspase 3	Mouse anti-caspase 3	Cell Signaling
Egr1	Rabbit anti-Egr1 (588)	Santa Cruz
γH2AX	Rabbit anti-γH2Ax	Novus Biologicals
pH3-Ser10	Rabbit anti-Histone H3 pSerine10	Millipore
Myc	Rabbit anti-c-Myc (Y69)	AbCam
CAD	Rabbit anti-DFFB	Sigma
HRP anti-sheep/ mouse/ rabbit	Conjugated secondaries	Invitrogen
ICAD	Rabbit anti-ICAD	AbCam
Mcl1	Rabbit anti-Mcl1 (S-19)	Santa Cruz Biotechnology
Myc epitope tag	4A6	Millipore
Noxa	Mouse anti-Noxa (114C307)	Merck Millipore
Tao1	Sheep anti-Tao1	(Westhorpe et al., 2010)
XIAP	Rabbit anti-XIAP	Cell Signaling Technology

Small molecule inhibitors

Small molecule inhibitors were dissolved in DMSO and stored at -20^{o}C, except tetracycline which was dissolved in water.

Name	1^{o} Target	Concentration	Source/ Citation
AZ138	Eg5/KSP	1 μM	AstraZeneca (Gascoigne and Taylor, 2008)
AZ3146	Mps1	2 μM	AstraZeneca (Hewitt et al., 2010)
BI2536	Plk1	100 nM	Boehringer Ingelheim (Steegmaier et al., 2007)
GSK923295	Cenp-E	100 nM	(Wood et al., 2010), (Bennett et al., in preparation)
JQ1	Brd4	0.5 μM	Stefan Knapp (Filippakopoulos et al., 2010)
MLN8054	Aurora A	1 μM	Millennium Pharmaceuticals (Manfredi et al., 2007)
Nocodazole	Microtubules	30 ng/ml	Sigma
Taxol	Microtubules	100 nM	Sigma
Tetracycline	Tet repressor	See legends	Sigma
WEHI-539	Bcl-xL	100 nM	Apexbio (Lessene et al., 2013)
ZM447439	Aurora B	2 μM	Tocris (Ditchfield et al., 2003)

Supplemental References

Bunz, F., Dutriaux, A., Lengauer, C., Waldman, T., Zhou, S., Brown, J. P., Sedivy, J. M., Kinzler, K. W., and Vogelstein, B. (1998). Requirement for p53 and p21 to sustain G2 arrest after DNA damage. Science *282*, 1497-1501.

Chung, N., Zhang, X. D., Kreamer, A., Locco, L., Kuan, P. F., Bartz, S., Linsley, P. S., Ferrer, M., and Strulovici, B. (2008). Median absolute deviation to improve hit selection for genome-scale RNAi screens. J Biomol Screen *13*, 149-158.

Ditchfield, C., Johnson, V., Tighe, A., Ellston, R., Haworth, C., Johnson, T., Mortlock, A., Keen, N., and Taylor, S. S. (2003). Aurora B couples chromosome alignment with anaphase by targeting BubR1, Mad2, and Cenp-E to kinetochores. J Cell Biol *161*, 267-280.

Girdler, F., Gascoigne, K. E., Eyers, P. A., Hartmuth, S., Crafter, C., Foote, K. M., Keen, N. J., and Taylor, S. S. (2006). Validating Aurora B as an anti-cancer drug target. J Cell Sci *119*, 3664-3675.

Hewitt, L., Tighe, A., Santaguida, S., White, A. M., Jones, C. D., Musacchio, A., Green, S., and Taylor, S. S. (2010). Sustained Mps1 activity is required in mitosis to recruit O-Mad2 to the Mad1-C-Mad2 core complex. J Cell Biol *190*, 25-34.

Huang da, W., Sherman, B. T., and Lempicki, R. A. (2009). Systematic and integrative analysis of large gene lists using DAVID bioinformatics resources. Nat Protoc *4*, 44-57.

Karlseder, J., Smogorzewska, A., and de Lange, T. (2002). Senescence induced by altered telomere state, not telomere loss. Science *295*, 2446-2449.

Laoukili, J., Kooistra, M. R., Bras, A., Kauw, J., Kerkhoven, R. M., Morrison, A., Clevers, H., and Medema, R. H. (2005). FoxM1 is required for execution of the mitotic programme and chromosome stability. Nat Cell Biol *7*, 126-136.

Manfredi, M. G., Ecsedy, J. A., Meetze, K. A., Balani, S. K., Burenkova, O., Chen, W., Galvin, K. M., Hoar, K. M., Huck, J. J., LeRoy, P. J.*, et al.* (2007). Antitumor activity of MLN8054, an orally active small-molecule inhibitor of Aurora A kinase. Proc Natl Acad Sci U S A *104*, 4106-4111.

Soucek, L., Helmer-Citterich, M., Sacco, A., Jucker, R., Cesareni, G., and Nasi, S. (1998). Design and properties of a Myc derivative that efficiently homodimerizes. Oncogene *17*, 2463-2472.

Steegmaier, M., Hoffmann, M., Baum, A., Lenart, P., Petronczki, M., Krssak, M., Gurtler, U., Garin-Chesa, P., Lieb, S., Quant, J.*, et al.* (2007). BI 2536, a potent and selective inhibitor of polo-like kinase 1, inhibits tumor growth in vivo. Curr Biol *17*, 316-322.

Supek, F., Bosnjak, M., Skunca, N., and Smuc, T. (2011). REVIGO summarizes and visualizes long lists of gene ontology terms. PLoS ONE *6*, e21800.

Taylor, S. S., Hussein, D., Wang, Y., Elderkin, S., and Morrow, C. J. (2001). Kinetochore localisation and phosphorylation of the mitotic checkpoint components Bub1 and BubR1 are differentially regulated by spindle events in human cells. J Cell Sci *114*, 4385-4395.

Westhorpe, F. G., Diez, M. A., Gurden, M. D., Tighe, A., and Taylor, S. S. (2010). Re-evaluating the role of Tao1 in the spindle checkpoint. Chromosoma *119*, 371-379.

Wood, K. W., Lad, L., Luo, L., Qian, X., Knight, S. D., Nevins, N., Brejc, K., Sutton, D., Gilmartin, A. G., Chua, P. R.*, et al.* (2010). Antitumor activity of an allosteric inhibitor of centromere-associated protein-E. Proc Natl Acad Sci U S A *107*, 5839-5844.

Yang, W., Soares, J., Greninger, P., Edelman, E. J., Lightfoot, H., Forbes, S., Bindal, N., Beare, D., Smith, J. A., Thompson, I. R.*, et al.* (2013). Genomics of Drug Sensitivity in Cancer (GDSC): a resource for therapeutic biomarker discovery in cancer cells. Nucleic Acids Res *41*, D955-961.